JOURNAL OF MATERIALS SCIENCE 24 (1989) 1974–1978

Internal friction, crack length of fracture origin and fracture surface energy in alumina–zirconia composites

T. ONO*, K. NAGATA‡, M. HASHIBA‡, E. MIURA‡, Y. NURISHI‡
Department of Physics, ‡Department of Chemistry, Faculty of Engineering, Gifu University, Gifu 501-11, Japan

T. SHIMADA
Gifu Prefectural Research Institute of Ceramics, Gifu, Japan

Two series of alumina–zirconia composites, i.e. alumina–unstabilized zirconia and alumina–partially stabilized zirconia with 3 mol% Y_2O_3, with different zirconia content were slip casted and fired at 1550° C for 3 h. Elastic constant, bending strength and fracture toughness were measured. Internal friction was determined to follow the formation of cracks, nondestructively, which could be one of the fracture origins. The crack length of the fracture origin and the fracture surface energy were calculated by applying Griffith's fracture theory. Microstructures of the fracture surfaces were observed using a scanning electron microscope. For the unstabilized zirconia system, the increase in the internal friction of the order from 10^{-4} to 10^{-3} was a guide to find the formation of cracks which lead to the fracture. The increase in the cracks becoming a fracture origin lead to the increase in K_{Ic} and also to the apparent increase in the fracture surface energy. For the partially stabilized zirconia system, the increase in the fracture surface energy with an increase in zirconia content, keeping low internal frictions of the order of 10^{-4}, indicates the intrinsic strengthening of the grain boundaries in comparison to the unstabilized zirconia system. Internal friction is the most suitable nondestructive physical quantity to find the microcracks which leads to the fracture.

1. Introduction

When tough ceramics are manufactured they are expected to have strong bending strength and high fracture surface energy.

Griffith's fracture mechanics indicates that the tough material should have a high bending strength under identical crack size from Equation 1 [1].

$$\sigma_f = \frac{K_{Ic}}{Y C^{1/2}} \quad (1)$$

where

$$K_{Ic} = (2E \cdot \Gamma)^{1/2} \quad (2)$$

σ_f is the bending strength, K_{Ic} the fracture toughness, Y the shape factor of the crack, C the crack length of fracture origin, E the elastic constant and Γ the fracture surface energy. And also the tough material should have a high fracture surface energy for the material having an equivalent elastic constant from Equation 2.

Two toughening mechanisms, i.e. transformation toughening [2, 3] and microcracking [4, 5], have been introduced to explain the toughening of ZrO_2 dispersed ceramics. In either cases, once the transformation has occurred, there is a possibility of formation of microcracks in the body.

It is necessary to find the optimum conditions so as not to reduce the bending strength brought about by the growth of the microcracks and also not to result in an apparent increase in the fracture surface energy by reducing the elastic constant due to microcracking. Internal friction is a guide to judge whether cracks are in the body or not.

Alumina–unstabilized zirconia and alumina–partially stabilized zirconia with different zirconia content have been examined for toughness and bending strength by Green [5], Lange [2] and Tsukuma *et al.* [6]. An identical processing condition is, however, necessary to compare the values for the different series of composites [7].

Two series of alumina–zirconia composites with different zirconia content were prepared under identical processing conditions by slip casting.

Elastic constant, bending strength and fracture toughness of those samples were determined to calculate the crack length of fracture origin and the fracture surface energy by applying Equations 1 and 2. Also the internal friction of those samples was measured so as to follow the formation of microcracks nondestructively. The microstructure of the fracture surfaces was observed by using a scanning electron microscope (SEM).

In order to find if the formation of cracks is a fracture origin and make clear the apparent increase in the fracture surface energy, effectiveness of the measurement of internal friction was discussed.

0022–2461/89 $03.00 + .12

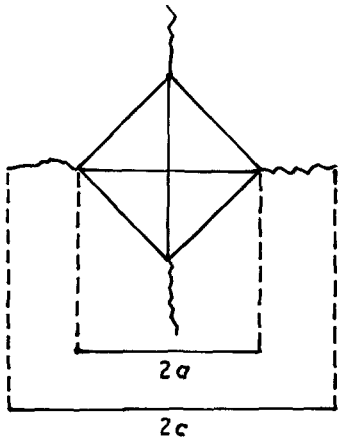

Figure 1 Size of diagonal of Vicker's indentation and crack length.

2. Experimental procedure

2.1. Materials and preparation of samples

Alumina powder used in this study is Alcoa A-16 α-Al_2O_3 of average particle size 0.3 μm. The sources of zirconia are Toyo Soda TZ-3Y (TSK Co., Sinnanyo, Yamaguchi, 746, Japan) for the tetragonal form of partially stabilized zirconia with 3 mol % yttrium oxide (to be described below as 3Y–PSZ) and Daiichi Kigenso EP zirconia (Daiichi Kigenso Chemicals Co., Osaka, Japan) for the monoclinic form of unstabilized zirconia (to be described as EP-ZrO_2).

Alumina–zirconia powders of various compositions were milled for 3 days with 1% dispersant, Celuna D-305 (Chukyo Yushi Co., Nagoya, 454, Japan), and formed by slip casting in a rectangular mould (4 mm by 10 mm by 80 mm).

Cast samples were heated at 1550° C for 3 h.

2.2. Measurements

Bending strength was obtained by the three-point bending test using a 3 cm span at a cross head speed of 1.7×10^{-3} m sec^{-1}.

Fracture toughness was determined for polished specimens using a microindentation technique under a load of 1 kg developed by Marshall and Evans [8] as shown in Equation 3.

$$K_{Ic} = 0.036E^{0.4}P^{0.6}a^{-0.7}(c/a)^{-1.5} \quad (3)$$

where K_{Ic} is the fracture toughness (MPa m$^{0.5}$); P the load (N); E the Young's modulus; a the half length of the diagonal indented on samples; c the length from the centre of the diagonal to the front of the crack grown from the top of the diagonal as shown in Fig. 1.

Young's modulus, E, was measured at room temperature by the flexural resonance technique and calculated from Equation 4.

$$E = \frac{48\,\pi^2 \varrho l^4 f_0^2}{m^4 a^2} \quad (4)$$

where ϱ is bulk density; l the length of specimen; f_0 the resonant frequency; m a constant determined from equation for flexural vibration, which is equal to 4.73 at the fundamental mode.

Internal friction is expressed generally by the ratio of loss energy ΔW to vibration energy per cycle. In this experiment, internal friction Q^{-1} was calculated from Equation 5 using the half value width Δf of a resonance curve as discussed elsewhere [9].

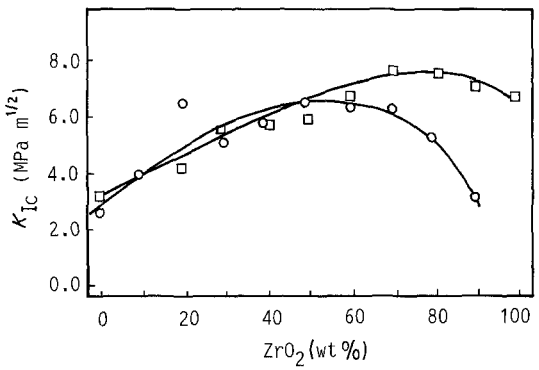

Figure 2 Fracture toughness of alumina–zirconia composites. (□) Al_2O_3–3Y–PSZ; (○) Al_2O_3–EP–ZrO_2.

$$Q^{-1} = \frac{\Delta f}{3^{1/2} f_0} \quad (5)$$

The fractions of monoclinic form, $f_{m\text{-}ZrO_2}$, and tetragonal form, $f_{t\text{-}ZrO_2}$, in zirconia phases, were calculated from the intensity of the X-ray diffraction peaks from (1 1 1) and (1 1 $\bar{1}$) lattice interfaces of monoclinic zirconia and from the (1 1 1) interface of tetragonal zirconia following Adam's method using Equations 5 and 6 [10, 11].

$$f_{m\text{-}ZrO_2} = \frac{I_m(1\,1\,1) + I_m(1\,1\,\bar{1})}{I_m(1\,1\,1) + I_t(1\,1\,1) + I_m(1\,1\,\bar{1})}$$
$$f_{t\text{-}ZrO_2} = \frac{I_t(1\,1\,1)}{I_m(1\,1\,1) + I_t(1\,1\,1) + I_m(1\,1\,\bar{1})} \quad (6)$$

where I_m and I_t express the intensity of each diffraction peaks.

2.3. Observation of microstructure

Microstructures were observed on fractured surfaces using a scanning electron microscope (SEM).

3. Results and discussions

3.1. Composition dependence of fracture toughness, bending strength, elastic constant and internal friction and form of zirconia

Fracture toughness measured for alumina–unstabilized ZrO_2 and alumina–3Y–PSZ composites are shown in Fig. 2. Addition of either form of zirconia to alumina resulted in a toughening effect. Both systems showed a maximum of the fracture toughness at 70 wt % zirconia for the 3Y–PSZ system and at 50 wt % zirconia for unstabilized zirconia system, respectively.

For the unstabilized zirconia system, reduction of the bending strength started at 20 wt % zirconia to about 200 MPa with a sharp decrease in elastic constant as shown in Fig. 3a. This value was heat constant for the successive increase in zirconia content to 80 wt %, but a further decrease was observed above 90 wt %. An abrupt increase in the internal friction from the order of 10^{-4} to 10^{-3} above 20 wt % zirconia was accompanied by the decrease in bending strength as also shown in Fig. 3a. The increase in the internal friction and also the decrease in the elastic constant with increase in unstabilized zirconia content indicated the formation of microcracks in the body as pointed out by Green [5]. The results of the X-ray diffraction shown in Fig. 4 indicates that the tetragonal

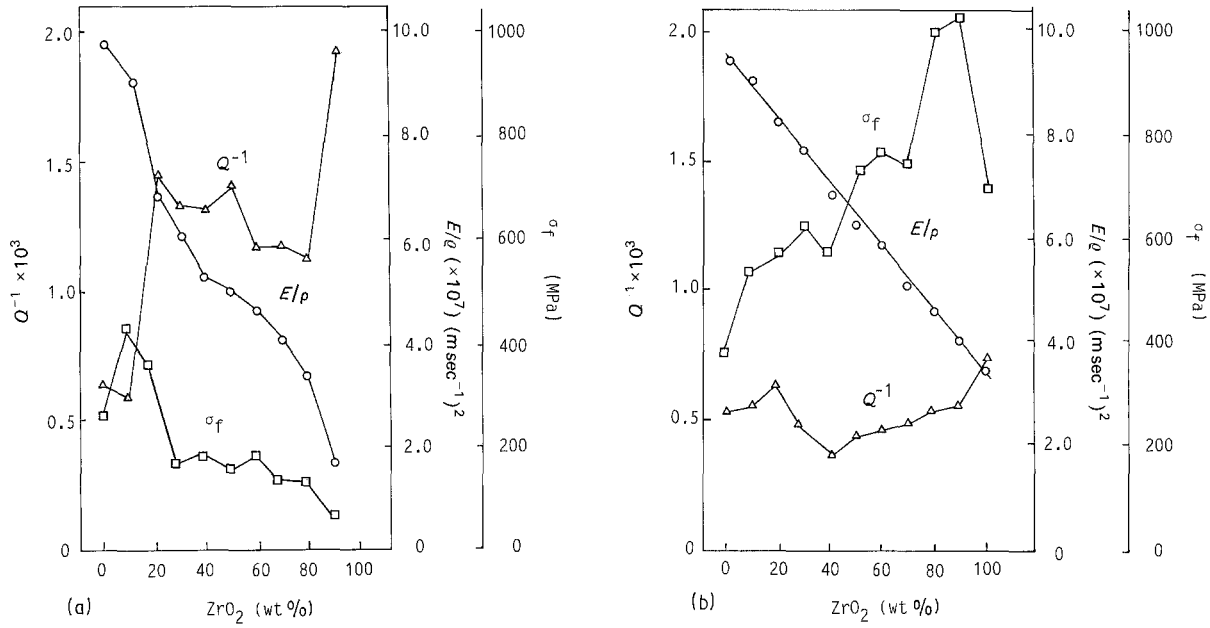

Figure 3 Composition dependence of bending strength, specific elastic constant and internal friction of alumina–zirconia composites: (a) alumina–unstabilized zirconia (EP–ZrO_2); (b) alumina–partially stabilized zirconia (3Y–PSZ) fired at 1550° C for 3 h.

form was unstable for the increase in zirconia content and disappeared in the region above 30 wt % zirconia. At least the toughening in the region of 30 to 50 wt % zirconia can only be explained by the microcracking theory [4, 5] because of the lack of the tetragonal form.

For the 3Y–PSZ system shown in Fig. 3b, the bending strength was increased and gave a maximum at 90 wt % zirconia accompanying with almost linear decrease in the elastic constant with increase of zirconia content. Under 30 wt % zirconia a small amount of zirconia, i.e. about 10 wt %, was transformed to the monoclinic form as shown in Fig. 4b. The reduction of the bending strength, however, did not occur in this region. Above 70 wt % zirconia the fraction of the monoclinic form was increased with increasing zirconia content. The tetragonal form is stable in the range from 40 to 60 wt % zirconia. The monoclinic form was not found in this range. The increase in the fraction of the monoclinic form did not necessarily result in the reduction of the bending strength for the partially stabilized system. The increase in toughness by the addition of partially stabilized zirconia under 70 wt % zirconia is possible by both or either of the transformation toughening [2, 3] and also the microcracking toughening [4, 5] without reducing the bending strength. In the range of 70 to 90 wt % zirconia the bending strength is increased in spite of the decrease in the fracture toughness. This falls short of the expectation from the Griffith theory [1] that the tough materials should be strong in bending strength. There should be a difference between the fracture using the bending test and the fracture using the development of the crack in the Vicker's indentation test. Internal friction for the 3Y–PSZ system showed low values in the order of 10^{-4} for all compositions.

3.2. Observation of microstructures

Figure 5 shows the position of the fracture origin observed by an optical microscope after the bending test. In the series of the unstabilized zirconia the fracture origin was indistinct above 20 wt % zirconia. Such a sample shows an intergranular fracture as shown in Fig. 6a. Under 20 wt % zirconia the fracture origin is located on the surface or the edge of the samples. And the fracture surface showed a mixed texture of the intergranular and intragranular fracture of alumina grains as seen in the microstructure of pure alumina shown in Fig. 6b.

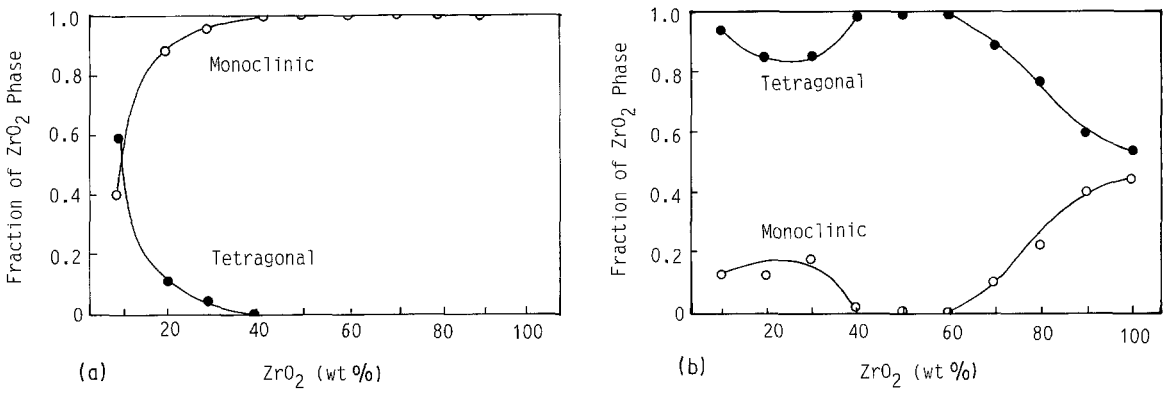

Figure 4 Composition dependence of the stability of tetragonal form of zirconia: (a) alumina–unstabilized zirconia (EP–ZrO_2); (b) alumina–partially stabilized zirconia (3Y–PSZ) fired at 1550° C, 3 h.

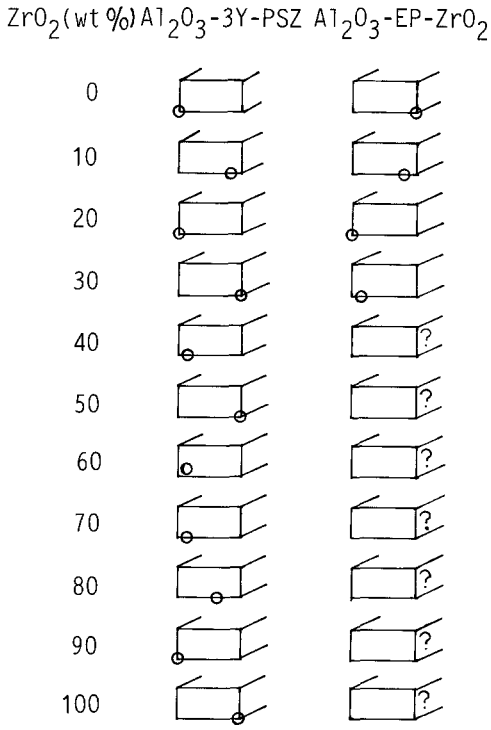

Figure 5 Location of fracture origin seen under an optical microscope after bending test for alumina–unstabilized zirconia and alumina–partially stabilized zirconia composites of different composition. Discerned position of fracture origin (○); undiscerned (?)

In the series of 3Y–PSZ the fracture origin was found on the surface of the samples irrespective of the zirconia content and the edge of the samples has an especially high probability as being the sources of the fracture origin. And the microstructure of the fracture surface showed an intragranular fracture as shown in Fig. 6c.

3.3. Calculation of the crack length of the fracture origin

The ratio of the bending strength of the alumina–zirconia composites to that of alumina is given in Equation 7.

$$\sigma_f/\sigma_{fA} = \frac{K_{Ic}/K_{IcA}}{(Y^2C/Y_A^2C_A)} \quad (7)$$

Therefore,

$$Y^2C/Y_A^2C_A = \left(\frac{K_{Ic}/K_{IcA}}{\sigma_f/\sigma_{fA}}\right)^2 \quad (8)$$

The value, $Y^2C/Y_A^2C_A$ including the ratio of the square of the shape factor of fracture origin is designated as the normalized crack length of the fracture origin. For the identical shape of the fracture origin the ratio Y^2/Y_A^2 is cancelled and the value of Equation 8 is reduced to the relative value of the crack length of the fracture origin. There is no guarantee of constancy of the shape factor for the change of composition. We used, therefore, the ratio including shape factor in Equation 8 as the normalized crack length of the fracture origin.

The normalized crack length for alumina–zirconia composites was shown in Fig. 7.

For the unstabilized zirconia system, the normalized crack length of the fracture origin was abruptly increased in two steps at 20 and 80 wt % zirconia. The zirconia content at which the growth of crack length occurred, i.e. at 20 and 80 wt % zirconia, agreed with that of the reduction of the bending strength and also with that of the increase in the internal frictions. This indicated that the cracks formed by the addition of unstabilized zirconia led the fracture as a fracture origin. The internal frictions informed the formation of the cracks which leads to the fracture nondestructively. Green indicated [5] that microcracks were formed in the alumina–zirconia composite by increasing zirconia content. The intergranular fracture and indistinct fracture origin above 20 wt % zirconia indicates that such cracks would be at grain boundaries in the body. The samples above 80 wt % zirconia had large cracks which could be observed by scanning electron microscopy and the microcracks must have

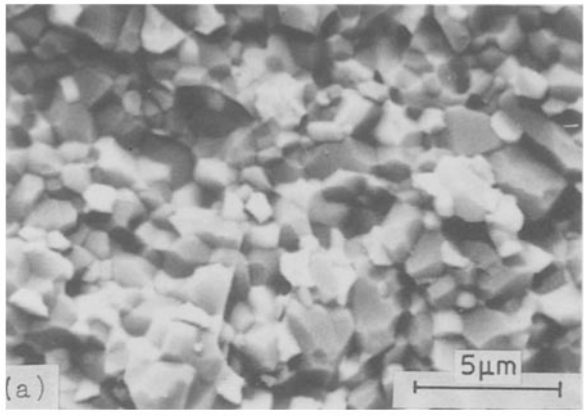

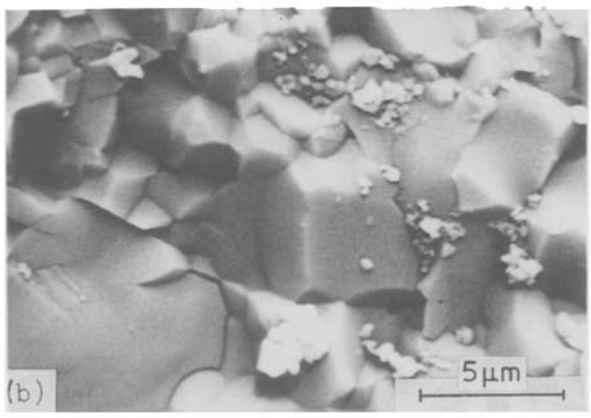

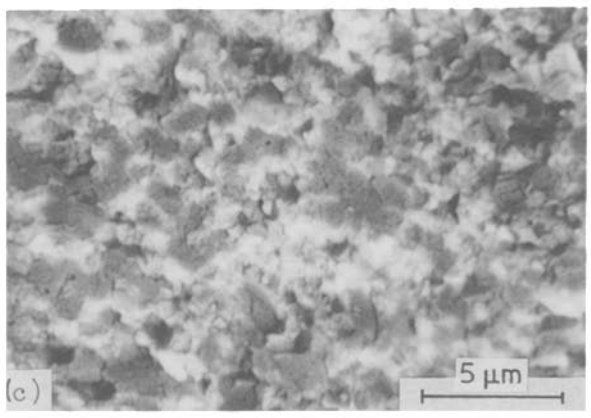

Figure 6 Microstructure of fracture surface near fracture origin: (a) alumina–unstabilized zirconia (30 wt % EP-ZrO_2); (b) alumina; (c) alumina–partially stabilized zirconia (60 wt % 3Y–PSZ).

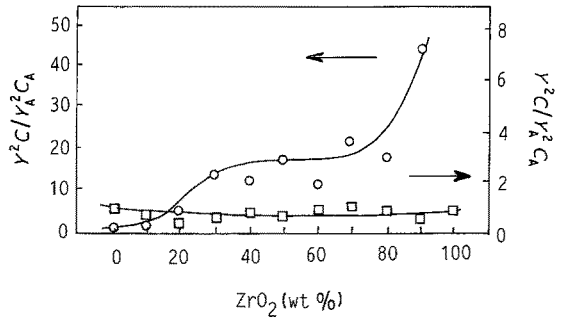

Figure 7 Normalized crack length of fracture origin. (□) Al_2O_3–3Y–PSZ; (○) Al_2O_3–EP–ZrO_2.

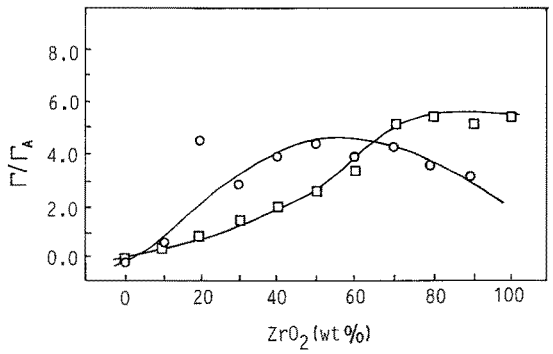

Figure 8 Normalized fracture surface energy. (□) Al_2O_3–3Y–PSZ; (○) Al_2O_3–EP–ZrO_2.

grown to a larger scale than in the region under 80 wt % zirconia.

For the 3Y–PSZ system, the normalized crack lengths of fracture origin were small. The bending strength increases with increase in zirconia content, as shown in Fig. 3. There are no signs of the crack formation which leads to the fracture in internal friction for the 3Y–PSZ systems. The addition of 3Y–PSZ to alumina strengthens the grain boundaries relative to that of the unstabilized zirconia system. Suppression of the transformation of zirconia from the tetragonal to monoclinic forms by partial stabilization must have suppressed the generation of cracks at the grain boundaries which weaken the texture.

3.4. Calculation of the fracture surface energy

The ratio of the fracture toughness of the composites to that of alumina is given in Equation 9.

$$(K_{Ic}/K_{IcA}) = \left(\frac{2E\Gamma}{2E_A\Gamma_A}\right)^{1/2} \quad (9)$$

The normalized fracture surface energy, (Γ/Γ_A) is defined by Equation 10.

$$(\Gamma/\Gamma_A) = (E_A/E)(K_{Ic}/K_{IcA})^2 \quad (10)$$

For 3Y–PSZ composites, the normalized fracture surface energy was increased with an increase in the zirconia content as shown in Fig. 8. There was no crack formation which led to the fracture. The increase in the normalized fracture surface energy with increase in zirconia content for the 3Y–PSZ system indicates the intrinsic increase in the bond strength of the mixture.

For the unstabilized system the normalized fracture surface energy also increased with the increase in zirconia content, having a maximum at 50 wt % zirconia which coincided with the maximum of the fracture toughness of the composites in spite of the reduction of the bending strength due to the generation of cracks above 20 wt % zirconia. The increase in the toughness above 20 wt % zirconia for the unstabilized system is based on the microcracking mechanism as described above. The increase in the normalized fracture surface energy with zirconia content is brought about by the increase in K_{Ic} and also the decrease in the elastic constant E following Equation 10 by microcrack formation. The increase in the fracture surface energy is, therefore, apparent.

4. Conclusions

Internal friction can give an indication of the crack formation which leads to the fracture for the alumina–unstabilized zirconia composites toughened by martensitic transformation of zirconia.

Microcrack formation by transformation of zirconia was characteristic for the alumina–unstabilized zirconia system and the formation of the microcracks during toughening gave an apparent increase in the fracture surface energy accompanied by a reduction in the bending strength and also a reduction of the elastic constant.

Alumina–partially stabilized zirconia with 3 mol % yttria showed no sign of the formation of microcracks in the internal friction which lead to fracture, and the increase in the fracture surface energy seen is due to intrinsic strengthening of the grain boundaries in comparison to unstabilized zirconia system.

References

1. D. W. RICHARDSON, in "Modern Ceramic Engineering" (Marcel Dekker, New York, 1982) p. 78 and p. 95.
2. F. F. LANGE, *J. Mater. Sci.* **17** (1982) 225.
3. N. CLAUSSEN, *J. Amer. Ceram. Soc.* **61** (1978) 85.
4. *Idem, ibid.* **59** (1976) 49.
5. D. J. GREEN, *ibid.* **65** (1982) 610.
6. K. TSUKUMA, K. UEDA and M. SHIMADA, *ibid.* **68** (1985) C-4.
7. T. SHIMADA, K. NAGATA, M. HASHIBA, E. MIURA, T. ONO and Y. NURISHI, in Abstract of the Annual Meeting of the Ceramic Society of Japan (Ceramic Society of Japan, Tokyo, 1985) p. 217.
8. D. B. MARSHALL and A. G. EVANS, *J. Amer. Ceram. Soc.* **64** (1981) C-182.
9. T. ONO, Y. NURISHI, M. HASHIBA and H. ITOH, *Jpn J. Appl. Phys.* **27** (1988) 1096.
10. E. D. WHITNEY, *J. C. S. Trans. Faraday Soc.* **61** (1965) 1991.
11. J. ADAM and B. COX, *J. Nuclear Energy, Part A, Reactor Science* **11** (1959) 31.

Received 24 March
and accepted 29 July 1988